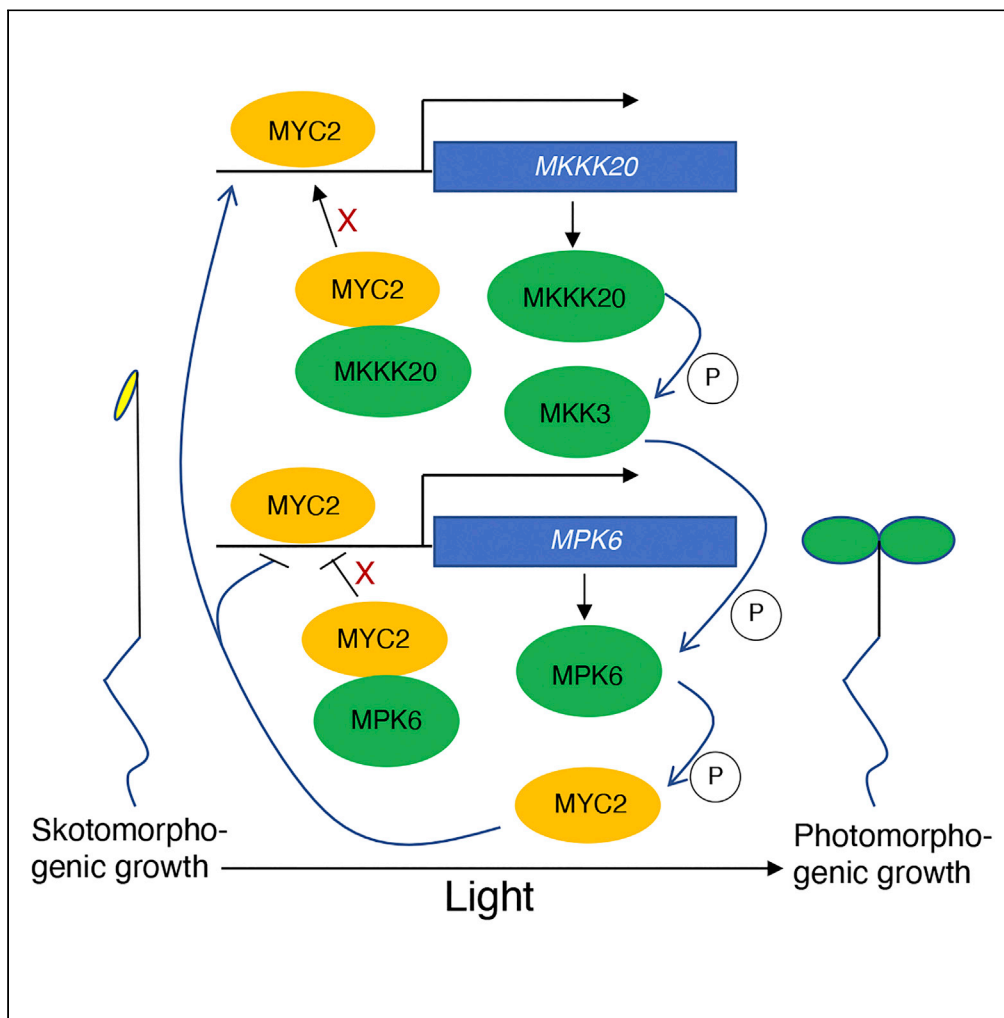Article

MKKK20 works as an upstream triple-kinase of MKK3-MPK6-MYC2 module in Arabidopsis seedling development

Madhusmita Ojha,
Deepanjali Verma,
Nibedita
Chakraborty, ...,
Neetu Verma,
Alok Krishna
Sinha, Sudip
Chattopadhyay

alok@nipgr.ac.in

Highlights

MKKK20 is the upstream kinase of MKK3-MPK6-MYC2 module in photomorphogenesis

MYC2-mediated promotion of *MKKK20* expression is nullified by MYC2-MKKK20 complex

MKKK20 and MYC2 work in a feedback loop mechanism in light signaling pathway

MYC2 regulates MKKK20-MKK3-MPK6 cascade in Arabidopsis seedling development

Article

MKKK20 works as an upstream triple-kinase of MKK3-MPK6-MYC2 module in Arabidopsis seedling development

Madhusmita Ojha,[1,5] Deepanjali Verma,[2,3,5] Nibedita Chakraborty,[1] Abhideep Pal,[1] Prakash Kumar Bhagat,[2,4] Anshuman Singh,[1] Neetu Verma,[2] Alok Krishna Sinha,[2,6,*] and Sudip Chattopadhyay[1]

SUMMARY

The mitogen-activated protein kinase (MAPK) cascade is involved in several signal transduction processes in eukaryotes. Here, we report a mechanistic function of MAP kinase kinase kinase 20 (MKKK20) in light signal transduction pathways. We show that MKKK20 acts as a negative regulator of photomorphogenic growth at various wavelengths of light. MKKK20 not only regulates the expression of light signaling pathway regulatory genes but also gets regulated by the same pathway genes. The *atmyc2 mkkk20* double mutant analysis shows that MYC2 works downstream to MKKK20 in the regulation of photomorphogenic growth. MYC2 directly binds to the promoter of *MKKK20* to modulate its expression. The protein-protein interaction study indicates that MKKK20 physically interacts with MYC2, and this interaction likely suppresses the MYC2-mediated promotion of *MKKK20* expression. Further, the protein phosphorylation studies demonstrate that MKKK20 works as the upstream kinase of MKK3-MPK6-MYC2 module in photomorphogenesis.

INTRODUCTION

Plant growth and development are regulated by several environmental factors, among which light signaling pathways play a central role. Plants have evolved with a variety of photoreceptor families that are involved in perception of various wavelengths and intensities of light, and subsequently transmit the information through downstream signaling components to regulate seedling development.[1–8] The transcriptional regulatory network plays an important role in light-mediated seedling development.[9,10]

Mitogen-activated protein kinase (MAPK) cascades are much conserved in eukaryotes, and are involved in several signal transduction processes.[11] In plants, MAPK pathways are reported to be involved in growth, programmed cell death, and various environmental cues including heat, cold, salinity, drought, UV rays, and pathogen attack.[12–20] The MAPK cascade is usually composed of a MAPK kinase kinase (MAPKKK), a MAPK kinase (MAPKK) and a MAPK, and it works via a phosphor-relay mechanism that links upstream receptors to downstream targets.[16,21]

MYC2 (a bHLH transcription factor) acts as a negative regulator of blue light-mediated photomorphogenic growth, and blue and far-red light-regulated gene expression.[22] MYC2 has been shown to bind to the G-box of *Suppressor of Phytochrome A1(SPA1)* promoter and regulates its expression during photomorphogenic growth.[23] MYC2 physically interacts with G-box binding bZIP transcription factor (GBF1) and works in an antagonistic manner in BL-mediated seedling development.[24] The *atmyc2* mutants have altered sensitivity to abscisic acid (ABA), jasmonic acid (JA) and ethylene-jasmonate mediated responses.[22,25–27] In addition, *atmyc2* mutants show increased resistance to leaf-infecting necrotrophic pathogens such as *Botrytis cinerea,* and the root-infecting pathogen *Fusarium oxysporum*.[25,27,28] Thus, MYC2 has emerged as a common regulator that cross-talks with multiple signaling pathways.

It has been shown by a protein microarray study that MKKK20 is able to interact with Calmodulin 7 (CAM7), which is a key transcription factor involved in light signaling pathways.[29–33] Further studies have revealed that whereas MPK6 works downstream of MKKK20 in the regulation of osmotic stress,[34] MKKK20 works upstream to MKK3 in the regulation of root growth.[35] The involvement of MKKK20 has been shown in ABA

[1]Department of Biotechnology, National Institute of Technology, Durgapur 713209, India

[2]National Institute of Plant Genome Research, Aruna Asaf Ali Marg, New Delhi 110067, India

[3]Present address: Department of Plant Biology, Rutgers, The State University of New Jersey, Piscataway, NJ 08901, USA

[4]Present address: School of Biological and Biomedical Sciences, Durham University, South Road, Durham DH1 3LE, UK

[5]These authors contributed equally

[6]Lead contact

*Correspondence: alok@nipgr.ac.in

https://doi.org/10.1016/j.isci.2023.106049

responses.[36] It has been shown that MKK5-MPK6 cascade works downstream to MKKK20 in this regulatory pathway.[36] Recent studies have shown that MYC2 and CAM7 work in an antagonistic manner in the regulation of *Elongated hypocotyl 5(HY5)* expression.[37] It has been reported that MYC2 supersedes the role of CAM7 to regulate *HY5*-promoter activity in Arabidopsis seedling development.[37] Although the light signal transduction pathways have well been studied, the direct connection of MAPK and light signaling pathways remains largely unknown. A recent study reveals that MKK3-MPK6 is activated by blue light in a MYC2 dependent manner.[38] MPK6 physically interacts and phosphorylates MYC2, and is phosphorylated by MKK3. Furthermore, MYC2 binds to *MPK6* promoter and regulates its expression in a feedback regulatory mechanism in blue light. Although the MKK3-MPK6-MYC2 module has been shown to be involved in blue light-mediated seedling development, the upstream triple kinase of this pathway remains unknown. In this study, we have functionally characterized MKKK20 as the triple kinase working upstream to MKK3-MPK6-MYC2 module in the regulation of photomorphogenic growth.

RESULTS

Analysis of *mkkk20* Mutant lines

In a protein microarray study, it has been shown that one of the upstream triple kinases, i.e., MKKK20 can interact with CAM7, which is a positive regulator of photomorphogenesis.[29,30] We ask whether MKKK20 plays any role in light-controlled seedling development. To address this question, we searched and obtained two transfer DNA mutant lines (SALK_124398 (*mkkk20-2*) and SALK_021755 (*mkkk20-1*)) from Arabidopsis Biological Resource Center, Ohio, USA.[39] The junctions of transfer DNA and *MKKK20* of *mkkk20-2* were amplified by PCR, and the DNA sequence analyses revealed that the transfer DNA was inserted in nucleotide position between +18 and +19 bp of the 5′ UTR region (Figures S1A–S1C). In another mutant line, *mkkk20-1*,[35] the transfer DNA was found to be inserted at nucleotide position between −34 bp and −35 bp of the promoter region of *MKKK20* (Figures S1F–S1H). The semiquantitative PCR and quantitative real-time PCR (qPCR) were performed to determine the transcript levels of *MKKK20* in these two mutant backgrounds. Both the mutant lines showed reduced transcript levels as compared to the corresponding wildtype background, indicating that both are knockdown mutant lines (Figure S1D, S1E,S1I, and S1J).

MKKK20 acts as a negative regulator of photomorphogenic growth

We grew wild type and *mkkk20* (*mkkk20-2 and mkkk20-1*) seedlings in dark and white light (WL) conditions. The 6-day-old *mkkk20-2 and mkkk20-1* seedlings did not show any significant difference in hypocotyl length as compared to wildtype in dark (Figures 1A, 1B and S2). However, the hypocotyl length of *mkkk20-2 and mkkk20-1* seedlings was found to be significantly shorter than that of wild type in WL (Figures 1A, 1B and S2). These results suggest that MKKK20 works as a negative regulator of photomorphogenic growth in WL. We then asked whether the altered photomorphogenic growth of *mkkk20-2* and *mkkk20-1* mutants was specific to a particular wavelength of light. To examine that, we grew the seedlings at various wavelengths of light and measured the hypocotyl length. The hypocotyl length of 6-day-old *mkkk20-2 and mkkk20-1* seedlings was found be significantly shorter in red light (RL), blue light (BL) and far-red light (FRL) conditions (Figures 1A, 1B and S2). Taken together, these results suggest that MKKK20 works as a negative regulator of photomorphogenic growth at various wavelengths of light. It is worth mentioning here that in subsequent experiments we used *mkkk20-2* mutant line for further studies.

Two physiological responses such as accumulation of chlorophyll and anthocyanin are modulated by multiple regulatory components of light signaling pathways.[22,40–42] To determine the possible role of MKKK20 on chlorophyll and anthocyanin accumulation, we determined the level of chlorophyll and anthocyanin accumulation in *mkkk20-2* mutant background. The level of chlorophyll accumulation was significantly increased in *mkkk20-2* as compared to wild-type background (Figure 1C). The level of anthocyanin was also found to be present at elevated level in *mkkk20-2* than the corresponding wildtype background (Figure 1D). Taken together, these results indicate that MKKK20 negatively regulates the accumulation of chlorophyll and anthocyanin.

MKKK20 regulates the expression of light signaling pathway genes

We then asked whether the expression of light inducible genes such as *Chlorophyll A/B binding protein 1* (*CAB1*), *Ribulose bis-phosphate carboxylase small chain 1A* (*RBCS-1A*) and *Chalcone synthase 1* (*CHS1*) was modulated by MKKK20. To test that, we performed qPCR to determine the steady state mRNA level of light
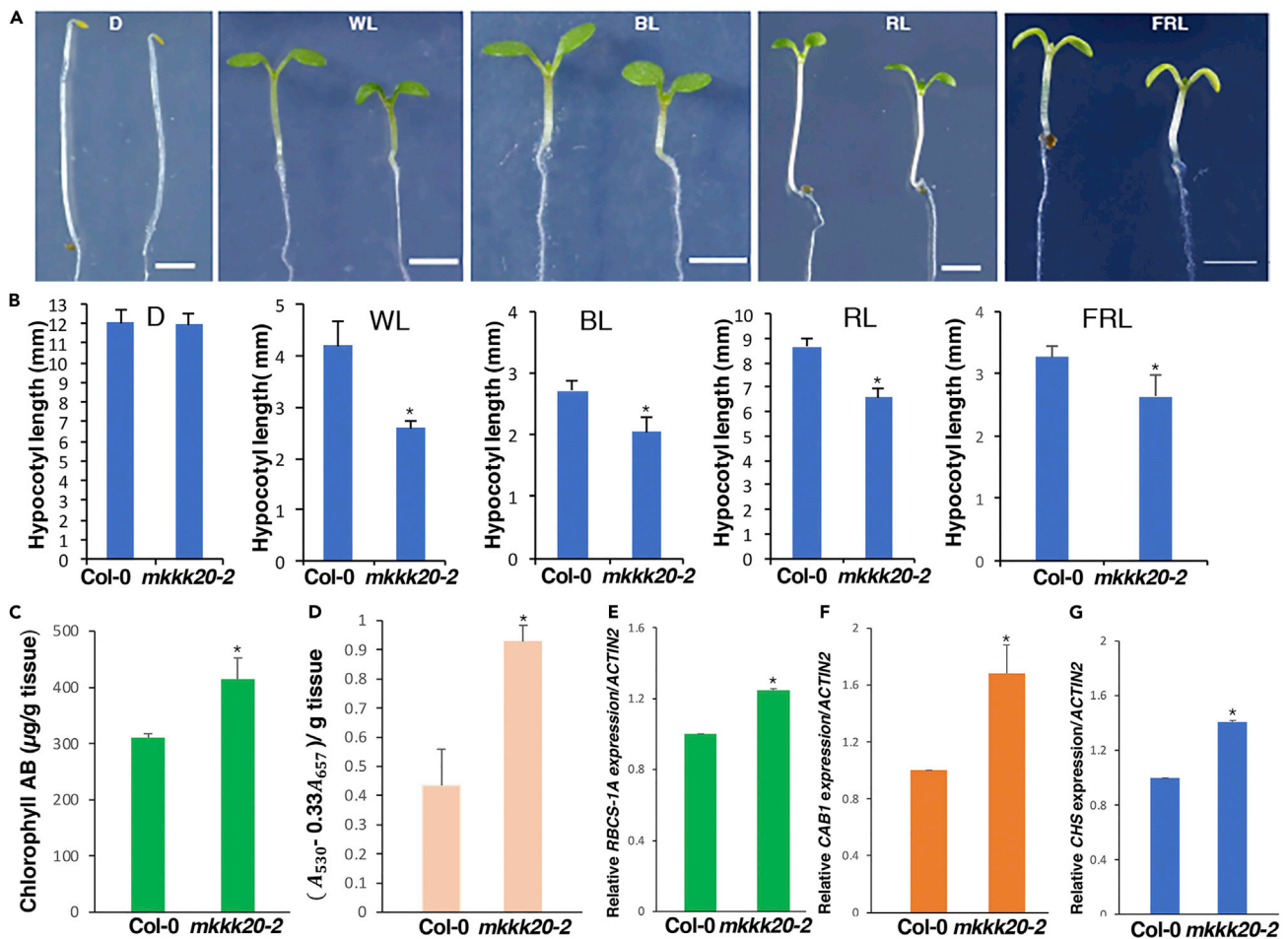
Figure 1. MKKK20 is a negative regulator of photomorphogenesis

(A) Phenotype of 6-day-old wild type (Col-0) (left side in each panel) and *mkkk20-2* mutant (right side in each panel) seedlings grown in constant dark (D), white light (WL:10 μmol/m^2/s^1), blue light (BL:20 μmol/m^2/s^1), red light (RL:20 μmol/m^2/s^1), or far-red light (FRL:1.5 μmol/m^2/s^1) conditions. Scale bar = 5 mm.

(B) Diagrammatic presentation of the mean (±SD; n = 15) values of hypocotyl length in Col-0 and *mkkk20-2* mutant seedlings grown in dark and at various wavelengths of light. The asterisk on the error bars indicates significant (pvalue <0.05) differences in hypocotyl length. The data were compared by using one-way ANOVA factorial analysis followed by Tukey's HSD test.

(C and D) Chlorophyll and anthocyanin contents, respectively, of 6-day-old wild type (Col-0) and *mkkk20-2* mutant seedlings grown under constant WL (30 μmol/m^2/s^1). Values (n = 3) are presented as Mean ± SEM of three biological replicates. Different small alphabetical letters on the error bars indicate significant (pvalue <0.05) differences of chlorophyll (C) and anthocyanin (D) in *mkkk20-2* mutants than wild type.

(E–G) Real-time PCR analysis of *RBCS-1A, CAB* and *CHS*, respectively in 6-day-old wild type (Col-0) and *mkkk20-2* mutant seedlings grown in WL (30 μmol/m^2/s^1). *ACTIN2* was used as internal control. Values (n = 3) are presented as Mean ± SEM of three biological replicates. The asterisk on the error bars indicates significant (pvalue <0.05) differences of *RBCS-1A, CAB1* and *CHS* transcripts in *mkkk20-2* than wild type. The data were compared by using one-way ANOVA factorial analysis followed by Tukey's HSD test.

inducible genes. The qPCR analyses revealed that all three light inducible genes tested had higher level of expression in *mkkk20-2* than the wildtype background (Figures 1E–1G).

We then selected a few genes working as positive or negative regulators of light signaling pathways and asked whether these genes such as *HY5, SPA1, GBF1* and *CAM7* were regulated by MKKK20. HY5, a positive regulator of photomorphogenesis, works in an antagonistic manner with MYC2 in Arabidopsis seedling development.[37] SPA1 acts as a repressor of photomorphogenesis and is genetically and molecularly interconnected with MYC2.[23] GBF1, a G-box binding bZIP transcription factor, plays an important role as both positive and negative regulator of photomorphogenesis; and it antagonistically works with MYC2 in blue light-mediated seedling development.[24,43] CAM7 is a positive regulator of photomorphogenesis that works in concert with HY5 and MYC2.[30,31,33,37] We performed qPCR analysis of 6-day-old WL grown
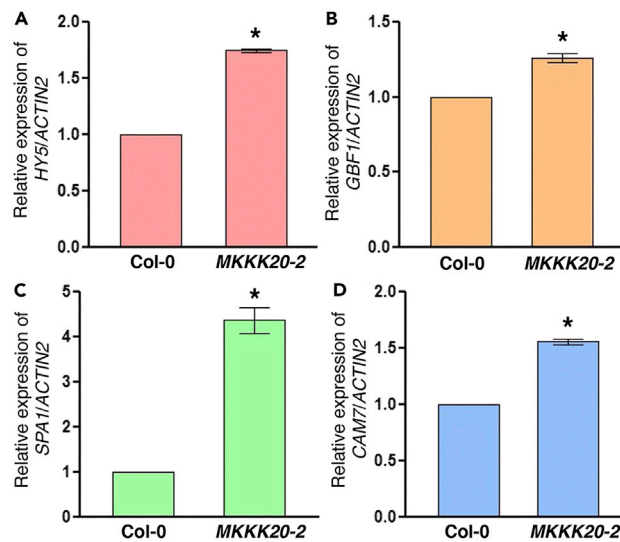
Figure 2. MKKK20 regulates the expression of regulatory genes of light signaling pathway
(A–D) Real-time PCR analyses of *HY5, GBF1, SPA1* and *CAM7*, respectively, in 6-day-old wild type (Col-0) and *mkkk20-2* mutant seedlings grown under constant WL (30 μmol/m^2/s^1). *ACTIN2* was used as an internal control. Values (n = 3) are presented as Mean ± SEM of three biological replicates. The asterisk on the error bars indicates significant (pvalue <0.05) differences of transcript levels in the *mkkk20-2*mutant compared to the wild type background. The data were compared by using one-way ANOVA factorial analysis followed by Tukey's HSD test.

seedlings; and the steady state mRNA level of these genes was estimated in wild type (Col-0) and *mkkk20-2* mutant seedlings. The level of expression of *HY5* (~1.5-fold), *SPA1* (~5-fold), *GBF1* (~1.3-fold) and *CAM7* (~1.5-fold) was found to be significantly higher in *mkkk20-2* mutant than the wildtype background. These results suggest that the expression of *HY5*, *SPA, GBF1* and *CAM7*is negatively regulated by MKKK20 (Figures 2A–2D).

MKKK20 regulates the flowering time and lateral root formation

Although propagating the *mkkk20-2* mutant plants in plant growth room chambers, it was observed that *mkkk2-2* plants flowered late as compared to wildtype plants. To determine the flowering time, we monitored the flowering time of *mkkk20-2* mutants under long day condition (14-h/10-h light/dark cycle) and compared with the wild type plants. As shown in Figure 3A, *mkkk20-2* plants had significantly delayed flowering time as compared to wildtype. Whereas wild type plants flowered with the formation of about 11 rosette leaves, *mkkk20-2* mutant plants flowered after more than 14 rosette leaves formed (Figure 3B). *FLOWERING LOCUS C (FLC)* encodes a MADS-box protein, which acts as a key repressor of inflorescence by negatively regulating the expression of genes such as *SUPPRESSOR OF OVEREXPRESSION OF CONSTANS 1 (SOC1)* and *FLOWERING LOCUS T* required to switch the meristem to a reproductive fate.[44–46] We wanted to examine whether MKKK20 affects the expression of *FLC*. The qPCR analysis of 6-day-old seedlings revealed that the expression of *FLC* was significantly elevated in *mkkk20-2* mutant as compared to wild type (Figures 3C and 3D), indicating that MKKK20 negatively regulates the expression of *FLC*. Examination of root growth of 16-day-old *mkkk20-2* mutant plants exhibited significantly lesser number of lateral roots as compared to wild type plants (Figure S3 A and B). These results suggest that MKKK20 acts as a positive regulator of flowering time and lateral root formation.

The expression of *MKKK20* is regulated by CAM7, HY5 and MYC2

CAM7 and HY5 are two transcription factors of photomorphogenesis that work in various wavelengths of light.[30,47] Both these proteins bind to the *HY5* promoter to regulate the expression of *HY5*. MYC2 competes with CAM7 to negatively regulate *HY5*-promoter activity in Arabidopsis seedling development.[37] Because *mkkk20* mutants display shorter hypocotyl phenotype at various wavelengths of light (Figure 1), we ask whether CAM7 and HY5 regulate the expression of *MKKK20*. We performed qPCR experiments using wild type, *cam7* and *hy5*mutant seedlings for this study. The transcript level of *MKKK20* was about
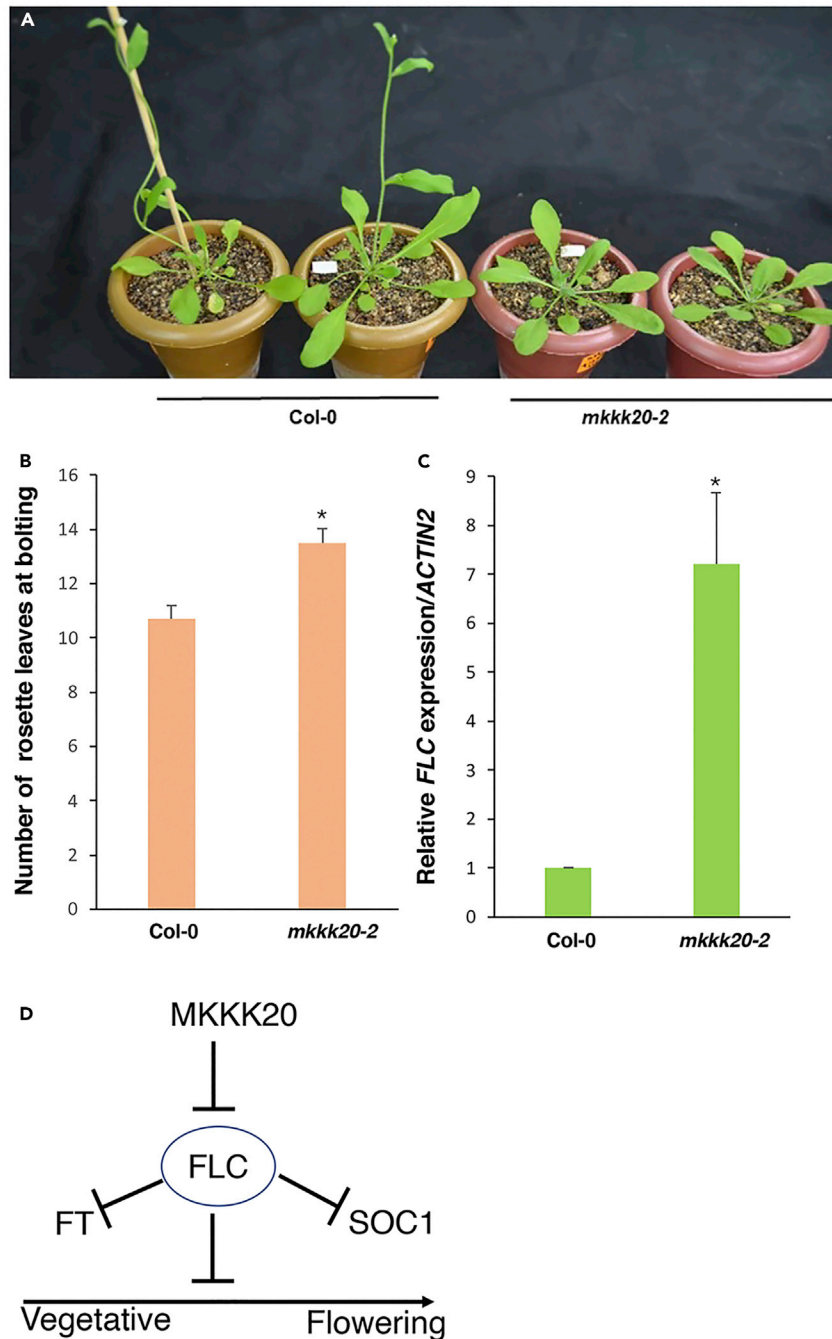
Figure 3. MKKK20 is involved in the regulation of flowering time

(A) The phenotype of 35-day-old wild type (Col-0) and *mkkk20-2* mutant plants grown in WL (100 µmol/m^2/s^1) under long day conditions (14h of light/10h of dark).

(B) Diagrammatic presentation of the mean ($\pm$SD = 15) values of number of rosette leaves produced at bolting in Col-0 and *mkkk20-2*. The asterisk on the error bars indicates significant (pvalue <0.05) differences in number of rosette leaves in *mkkk20-2* than the wild type.

(C) Real-time PCR analysis of *FLC* transcript level in 6-day-old wild type (Col-0) and *mkkk20-2* mutantseedlings grown in WL (30 µmol/m^2/s^1). *ACTIN2* was used as internal control. Values (n = 3) are presented as Mean $\pm$ SEM of three biological replicates. The asterisk on the error bars indicates significant (pvalue <0.05) differences of *FLC* transcript level in *mkkk20-2* mutant compared to the wild type (Col-0). The data were compared by using one-way ANOVA factorial analysis followed by Tukey's HSD test.

(D) A model showing the role of MKKK20 in the regulation of floral initiation by FLC, SOC1 and FT.
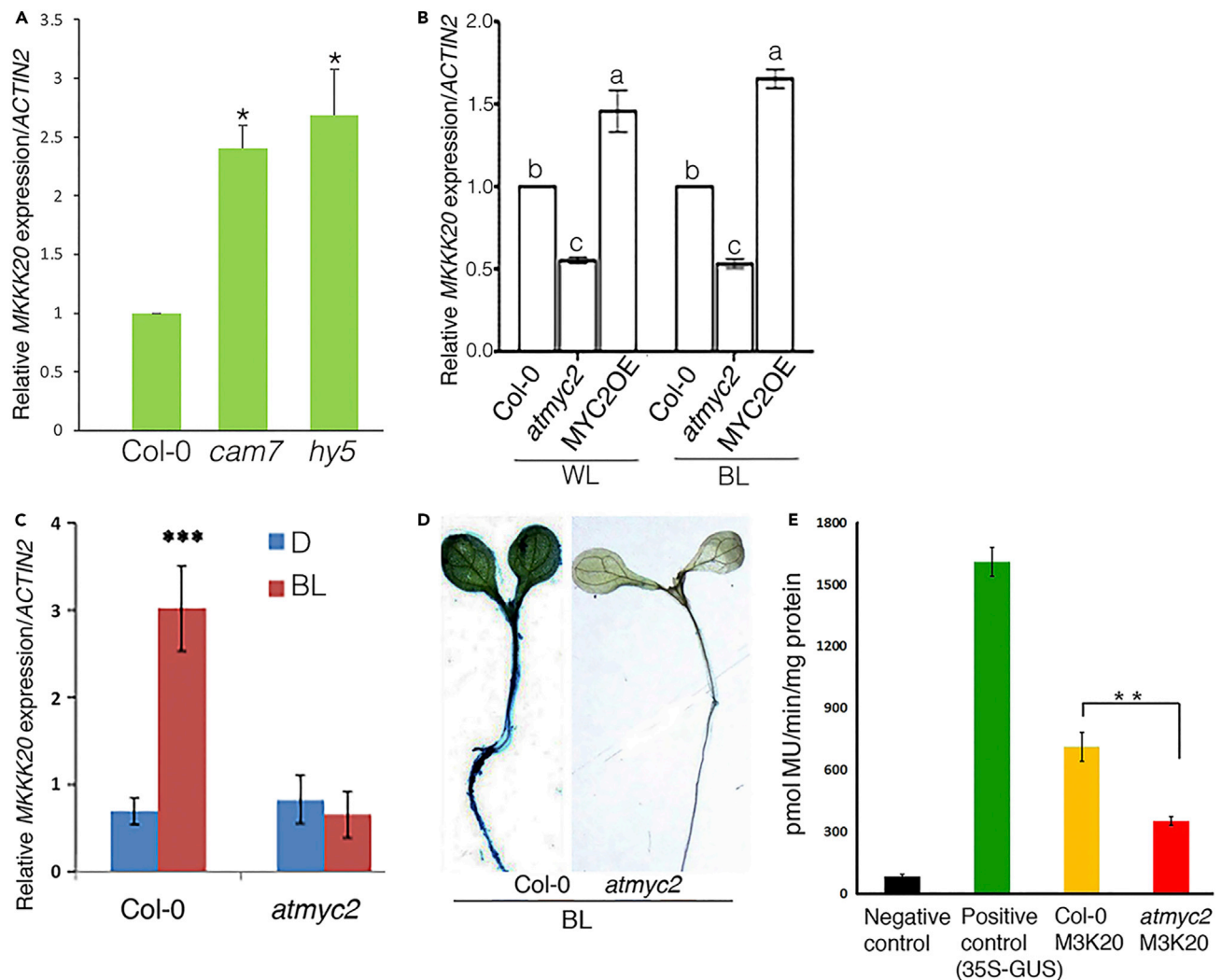
Figure 4. The expression of *MKKK20* is regulated by CAM7, HY5 and MYC2

(A) Real-time PCR analysis of *MKKK20* transcript level in 6-day-old wild type (Col-0), *cam7* and *hy5*mutant seedlings grown in WL (30 μmol/m^2/s^1). *ACTIN2* was used as internal control. Values (n = 3) are presented as Mean $\pm$ SEM of three biological replicates. The asterisk on the error bars indicates significant (pvalue <0.05) differences of *MKKK20* transcript level in *cam7* and *hy5* mutants compared to the wild type (Col-0).

(B) Real-time PCR analysis of *MKKK20* transcripts in 6-day-old wild type (Col-0), *atmyc2*mutant and MYC2OE seedlings grown in WL (30 μmol/m^2/s^1) and BL (20μmol/m^2/s^1) conditions. *ACTIN2* was used as internal control. Values (n = 2) are presented as Mean $\pm$ SEM of two biological replicates. Different small alphabetical letters on the error bars indicate significant (pvalue <0.05) differences of *MKKK20* transcript level in *atmyc2*mutant and MYC2OE compared to the wild type (Col-0). The data were compared by using one-way ANOVA factorial analysis followed by Tukey's HSD test.

(C) Transcript analysis of *MKKK20* in 6-day-old dark grown wild type (Col-0) and *atmyc2*mutant seedlings exposed to BL for 10 min. *ACTIN2* was used as internal control. Error bars represent SD (n = 3 independent experiments, with similar results). T-test was used to calculate significant (pvalue <0.0005) differences.

(D) Visualization of *GUS* expression driven by *MKKK20*promoter in 6-day-old BL grown wild type (Col-0) and *atmyc2*mutant seedlings.

(E) GUS fluorometric quantification assay showing *GUS* expression driven by *35S* and *MKKK20* promoters (*M3K20*) in 6-day-old BL grown wild type (Col-0) and *atmyc2*mutant seedlings. Asterisks indicate the significant difference in the activity of *MKKK20* promoter from wild type and *atmyc2*mutant (Student's *t* test, **p< 0.005).

2.5-fold higher in *cam7* and 2.7-fold higher in *hy5*mutant as compared to wildtype (Figure 4A), suggesting CAM7 and HY5 both negatively regulate the expression of *MKKK20*.

Earlier studies have shown that MYC2 negatively regulates the expression of *MPK6* and *MKK3,* and it works downstream of the MKK3-MPK6 cascade specific to BL signaling pathways.[38] Recent studies have shown that MKK3 physically interacts with MKKK20 to regulate the root microtubule functions.[35] Therefore, we

wanted to test the possible molecular connectivity between MYC2 and MKKK20. We first examined whether MYC2 regulated the expression of *MKKK20*. To test that, we monitored the expression of *MKKK20* in wild type, *atmyc2* and MYC2OE transgenic seedlings[24] grown in WL and BL through qPCR analysis. It was found that whereas the expression of *MKKK20* in *atmyc2* mutant was significantly reduced as compared to wildtype background, the expression level of *MKKK20* was significantly enhanced in MYC2 over-expressor (MYC2OE) background (Figure 4B). Thus, MYC2 is required for the optimum expression of *MKKK20*. We then examined the light induced expression of *MKKK20* in *atmyc2* background by transferring the seedlings from dark to BL. The seedlings were grown in constant dark for 6 days and then exposed to BL for 10 min. As shown in Figure 4C, the inducibility of *MKKK20* promoter activity was drastically reduced in *atmyc2* background as compared to wild type.

To further examine the above observations, we monitored the activity of *MKKK20* promoter in *atmyc2* mutant by transient expression analysis via GUS histochemical staining. Six-day-old wild type and *atmyc2* seedlings were transiently transformed to express the *GUS* reporter gene under the control of a 1.5-kb promoter sequence of *MKKK20*. In wild type seedlings, *GUS* was strongly expressed in all the organs tested, whereas in *atmyc2*, there was a drastic reduction in *GUS* expression (Figure 4D). We then performed GUS fluorometric quantification assay in Col-0 and *atmyc2* mutant lines and measured the activity of *MKKK20* promoter. Activation of *MKKK20* promoter was found to be significantly lower in *atmyc2* seedlings as compared to wild type (Figure 4E). These results altogether demonstrate that MYC2 positively regulates the expression of *MKKK20*.

MYC2 directly binds to the promoter of *MKKK20*

Because this study reveals that MYC2 positively regulates the expression of *MKKK20* either directly or indirectly, we wanted to examine whether MYC2 binds to the promoter of *MKKK20*. To investigate that, we first examined the DNA sequence of the promoter region of *MKKK20* and found a G-box (CACGTG) and an E-box (CATATG) in its promoter, which are located at −103 and −770 bp upstream to the transcriptional start site (Figure 5A). We carried out chromatin immunoprecipitation (ChIP) assays to examine *MKKK20* promoter and MYC2 interaction *in vivo*, using 6-day-old wild type (Col-0) and MYC2OE (which contains three copies of c-MYC epitopes fused to MYC2[48]) seedlings grown under constant BL ($30 \mu mol/m^2/s^1$). The qPCR analyses showed the enrichment of the G-box (∼2–fold) and E-box (∼1.5-fold) compared to the wild type (Figure 5B). However, no enrichment of the non-box (used as a control) was observed. These results suggest that MYC2 binds to the G-box and E-box of the *MKKK20* promoter *in vivo*.

We then performed Yeast-one hybrid assays to further examine the interaction of MYC2 with the G- and E-box of the *MKKK20* promoter. The protein (coding sequence of the gene) and promoter fragments were cloned in pGADT7 and pLacZi2μm vectors, respectively. The constructs were then co-transformed into the *EGY48* strain and grown on a defined double dropout (2D) medium devoid of leucine and uracil but supplemented with X-Gal substrate. The GAL4 activation domain-fused MYC2 (AD-MYC2) binds to the *MKKK20* promoter fragment containing the G and E-box, resulting in the *lacZ* reporter gene's induction, leading to the blue coloration of the transformed yeast colonies (Figures 5C and 5A). The mutated G-box (from CACGTG to AACGTT) with wild type E-box; and mutated E-box (from CATATG to TTATAA) with wild type G-box also result in blue coloration of yeast colonies that indicates the binding of MYC2 to the G-box and E-box (Figures 5C,5E, and 5F). However, the *MKKK20* promoter fragment containing both mutated G and E-box, and the other negative controls could not induce the reporter gene; hence, no coloration of the yeast cells (Figures 5C, 5B–5D and 5G–5J). Taken together, these results suggest that MYC2 directly binds to the G and E-box of the *MKKK20* promoter.

MKKK20 physically interacts with MYC2

Because the earlier study has revealed that MYC2 binds to the *MPK6* promoter and interacts with MPK6 in a feedback regulatory mechanism,[38] we ask whether MKKK20 and MYC2 physically interact with each other. To determine the physical interaction between MYC2 and MKKK20, we first carried out yeast two-hybrid protein-protein interaction study. For this experiment, the full length coding sequence (CDS) of MYC2 and CONSTITUTIVELY PHOTOMORPHOGENIC 1 (COP1) (as control) fused with GAL4 DNA-binding domain (BD-MYC2 and BD-COP1), and full length CDS of MKKK20 and HY5 were fused with GAL4 activating domain (AD-MKKK20 and AD-HY5). The protein-protein interaction between COP1 and HY5 was used as positive control.[47] The fusion constructs were co-transformed into yeast AH109 strain and observed the growth of co-transformed yeast cells on 2D (devoid of leucine and tryptophan) and 4D (devoid of leucine, tryptophan,
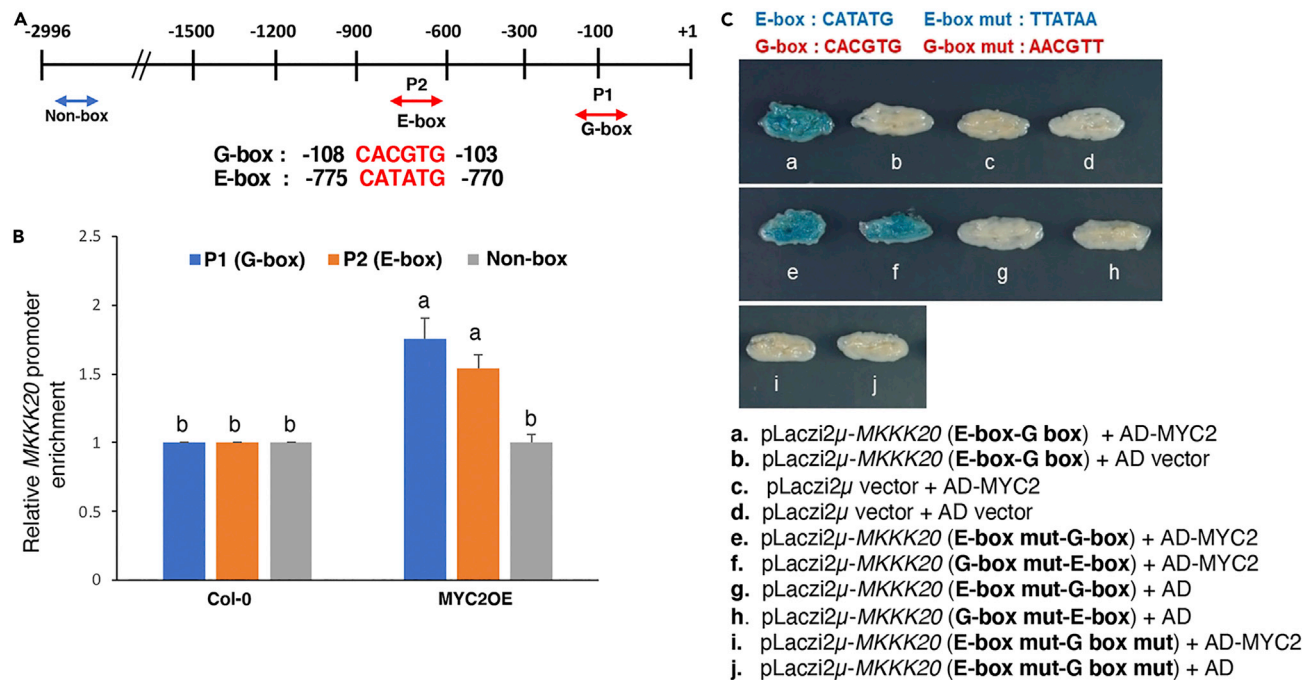
Figure 5. MYC2 binds to the promoter of *MKKK20*

(A) Schematic representation of *MKKK20* promoter fragment showing the positions of G- and E-box. The position (+1) indicates the transcriptional start site. The red arrows indicate the positions of DNA fragments used for ChIP assays. The blue arrow indicates the position of DNA fragment without any LRE (termed 'Non-box') used as negative control for ChIP assay.

(B) Chromatin immunoprecipitation (ChIP) assay of *MKKK20* promoter from 6-day-old BL (30 μmol/m^2/s^1)grown Col-0 and MYC2OE transgenic seedlings using antibodies to cMyc. The ChIP values were first normalized by their respective input values, and fold enrichment was then calculated relative to the wild-type. Values (n = 3) are presented as Mean $\pm$ SEM of three biological replicates. Different small alphabetical letters on the error bars indicate significant (pvalue <0.05) differences of *MKKK20* promoter enrichment in MYC2OE lines compared to the wild type (Col-0). The data were compared by using one-way ANOVA factorial analysis followed by Tukey's HSD test.

(C) Yeast one-hybrid interaction between *MKKK20* promoter fragment and MYC2 by co-transforming Yeast *EGY48* strain, and plating on double drop-out media (2D) devoid of leucine and uracil however supplemented with X-gal. Result of one representative experiment out of three has been shown.

adenine, histidine) plates. As shown in Figure 6A, MYC2 was able to interact with MKKK20. The empty vectors (AD and BD) and their respective combinations with MYC2 and MKKK20 used as negative controls were not able to interact. The COP1 and HY5, as expected, did interact with each other.[47]

To further substantiate the physical interaction between MYC2 and MKKK20, Bimolecular Fluorescence Complementation (BiFC) assay was performed. For this study, the CDS of MYC2 and MKKK20 were cloned into pSPYCE and pSPYNE vectors (MYC2-cYFP and MKKK20-nYFP), respectively. The MYC2-cYFP and ARR16-nYFP were used as positive control[48](Srivastava et al., 2019; PhD thesis title- Molecular and Functional Characterization of MYC2-Regulated ARR16 in *Arabidopsis thaliana*, submitted by Archana Kumari Srivastava at NIT Durgapur in 2018). The constructs were transformed into *Agrobacterium GV3101* strain, which then agroinfiltrated in onion epidermal cells for co-expression. Reconstituted YFP fluorescence was observed between MYC2-cYFP and MKKK20-nYFP (Figure 6B), whereas no YFP fluorescence was observed either in the empty vectors (cYFP + nYFP) or their respective combinations with MYC2 and MKKK20. A strong YFP fluorescence was also observed in MYC2-cYFP and ARR16-nYFP.[49] The pCAMBIA1303 was used as a transformation control. We further analyzed the interaction between MYC2 and other MKKKs (MKKK15 and MKKK16) (Figure S4) to test the specificity of interaction. However, no interaction of MYC2 was observed with MKKK15 and MKKK16, suggesting the specificity of interaction between MYC2 and MKKK20. Taken together, these results suggest that MYC2 physically interacts with MKKK20.

MYC2 and MKKK20 work in a common pathway of Arabidopsis seedling development

Because MYC2 binds to the promoter of *MKKK20* and also physically interacts with MKKK20, we wanted to determine the physiological relationship between *MYC2* and *MKKK20* through genetic studies. For this
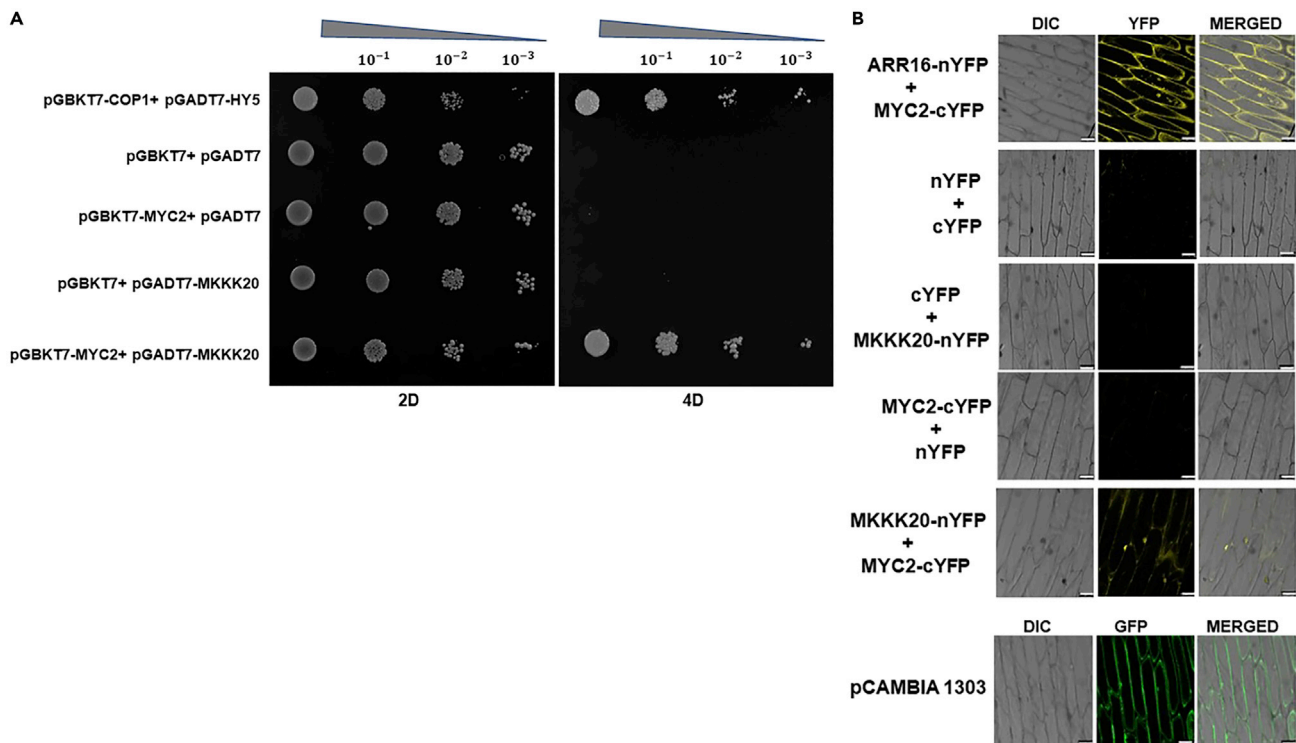
Figure 6. MKKK20 physically interacts with MYC2

(A)Yeast two-hybrid assay of full length MKKK20 and MYC2. Co-transformed yeast cells were grown in 2D (lacking Leu and Trp amino acids) and 4D (lacking Leu, Trp, Ade and His nutrients) selective media to test the protein-protein interactions. pGBKT7-COP1+ pGADT7-HY5 was used as positive control. The empty vectors (pGBKT7 and pGADT7) and their combinations with MKKK20 (pGBKT7 + pGADT7-MKKK20) and MYC2 (pGBKT7-MYC2 + pGADT7) were used as negative controls. Numbers above the panel indicate dilutions of the starting culture spotted on dropout media.

(B) The BiFC study of full length MKKK20-YFP[N−ter] (MKKK20-nYFP) and MYC2-YFP[C−ter](MYC2-c-YFP). Epifluorescence images of onion epidermal cells co-infiltrated with a mixture of *Agrobacterium* suspensions harboring constructs encoding the indicated fusion proteins. Bar represents 100 μm.

investigation, *mkkk20-2 atmyc2* double mutant plants were generated through genetic crosses. The homozygous *mkkk20-2*mutant plants were genetically crossed with *atmyc2-3*homozygous lines.[22] The homozygous *mkkk20-2atmyc2* double mutant plants were then used for further studies (Figure S5). We grew 6-day-old wild type (Col-0), *mkkk20-2, atmyc2*, and *mkkk20-2 atmyc2* seedlings in dark and WL conditions. The dark-grown seedlings of *mkkk20-2, atmyc2* and *mkkk20-2 atmyc2* mutants did not exhibit any significant difference in hypocotyl length compared to wild type seedlings (Figures 7A and 7D). Measurements of hypocotyl length of 6-day-old seedlings grown in WL revealed that the *mkkk20-2 atmyc2* double mutants exhibited significantly shorter hypocotyl length than each of the single mutants, suggesting that MKKK20and MYC2 work in an additive manner to control the hypocotyl length in WL (Figures 7B and 7E). Because *atmyc2* seedlings display shorter hypocotyl specifically in BL,[22–24] we examined the possible genetic interrelations between *atmyc2* and *mkkk20-2* in BL. The measurement of hypocotyl length of 6-day-old BL-grown seedlings revealed that the *mkkk20-2* and *atmyc2* mutants had shorter hypocotyl than the wild type. However, the hypocotyl length of *mkkk20-2 atmyc2* double mutant was found to be similar to *atmyc2* single mutant, suggesting that MYC2 and MKKK20 work in a common pathway to regulate the hypocotyl growth in BL (Figures 7C and 7F).

To examine whether MKKK20, MKK3, MPK6 and MYC2 work in the same branched pathway of light signal transduction, we examined the seedling growth of *mkkk20, mkk3, mpk6* and *atmyc2* mutant seedlings in WL and measured the hypocotyl length. As shown in Figures 7G and 7H, the mutant seedlings displayed similar hypocotyl length and shorter than the wild type. Taking together, these results indicate that MKKK20, MKK3, MPK6 and MYC2 work in a common pathway of light-mediated seedling development.
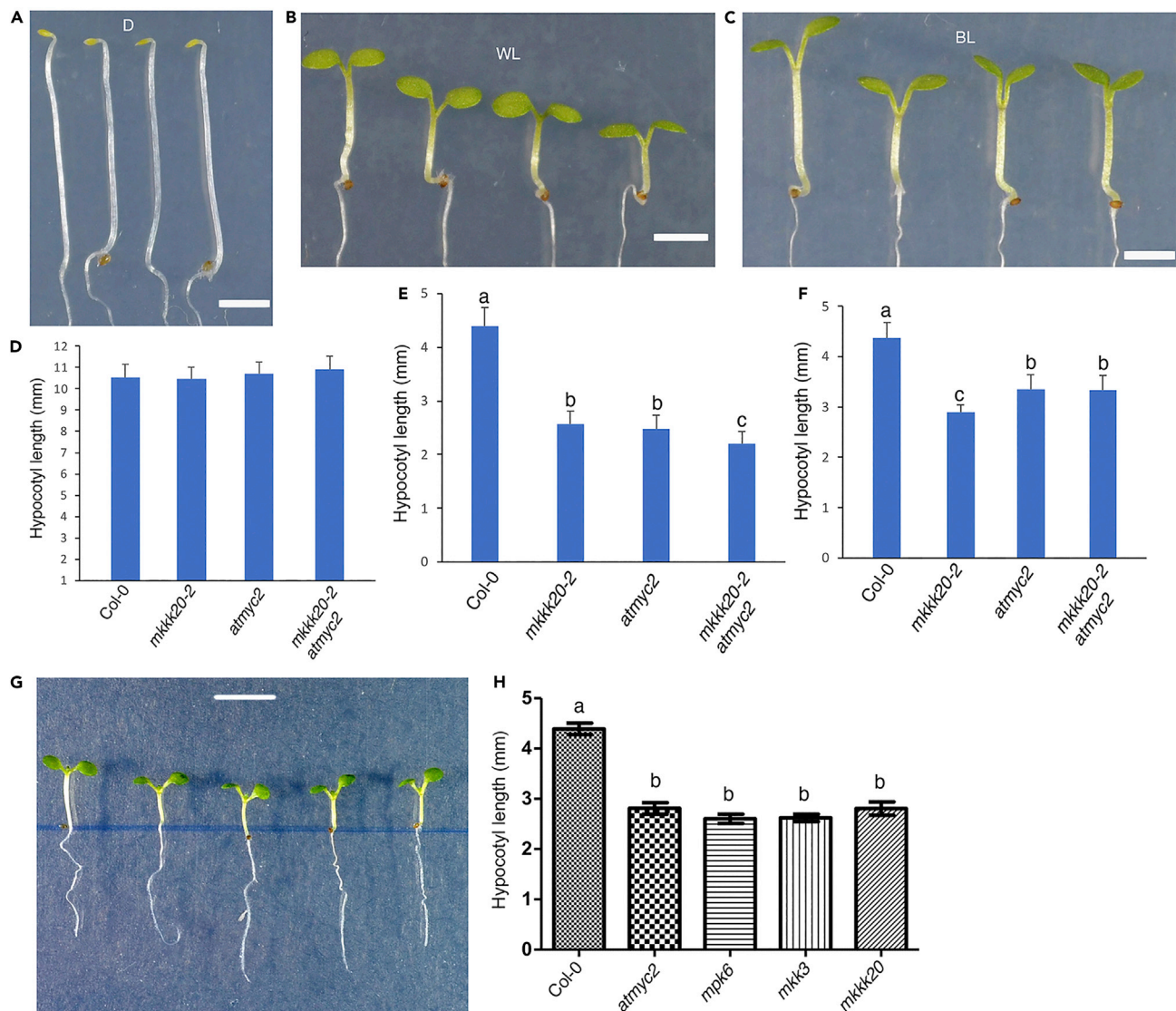
Figure 7. *MKKK20* genetically interacts with *MYC2*

(A–C) Phenotype of 6-day-old wild type (Col-0), *mkkk20-2*, *atmyc2* and *mkkk20-2 atmyc2* seedlings grown in dark (D), WL (10 μmol/m^2/s^1), and BL (10 μmol/m^2/s^1). Scale bar = 2 mm.

(D–F) Diagrammatic presentation of the mean (±SD; n = 15) values of hypocotyl length in different genotypes grown in dark, WL, and BL, respectively. Different small alphabetical letters on the error bars indicate significant (pvalue <0.05) differences in hypocotyl length. The data were compared by using one-way ANOVA factorial analysis followed by Tukey's HSD test.

(G) Phenotypic analysis of *mkkk20, mkk3, mpk6,* and *atmyc2* mutant seedlings. Phenotype of 6-day-old wild type (Col-0), *atmyc2, mpk6, mkk3* and *mkkk20-2* seedlings grown in WL (20 μmol/m^2/s^1).

(H) Diagrammatic presentation of the mean (±SD; n = 10) values of hypocotyl length in different genotypes grown in WL. Different small alphabetical letters on the error bars indicate significant (pvalue <0.05) differences in hypocotyl length. The data were compared by using one-way ANOVA factorial analysis followed by Tukey's HSD test. Bar = 5 mm.

MKKK20 affects the phosphorylation status and activity of MPK6 in blue light

MYC2 is part of the module of MKK3-MPK6-MYC2 involved in BL signaling pathways.[38] Considering the molecular and functional interconnection of MKKK20 and MYC2 in this study, we ask whether MKKK20 is the upstream regulator of MKK3-MPK6-MYC2 module. Recent studies have shown that MKKK20 physically interacts with MKK3.[35] To determine and further test the interaction observed in the previous report, we examined whether MKKK20 physically interacts with MKK3 in a yeast two-hybrid assay. As shown in Figure S6, MKK3 indeed can specifically interact with MKKK20.
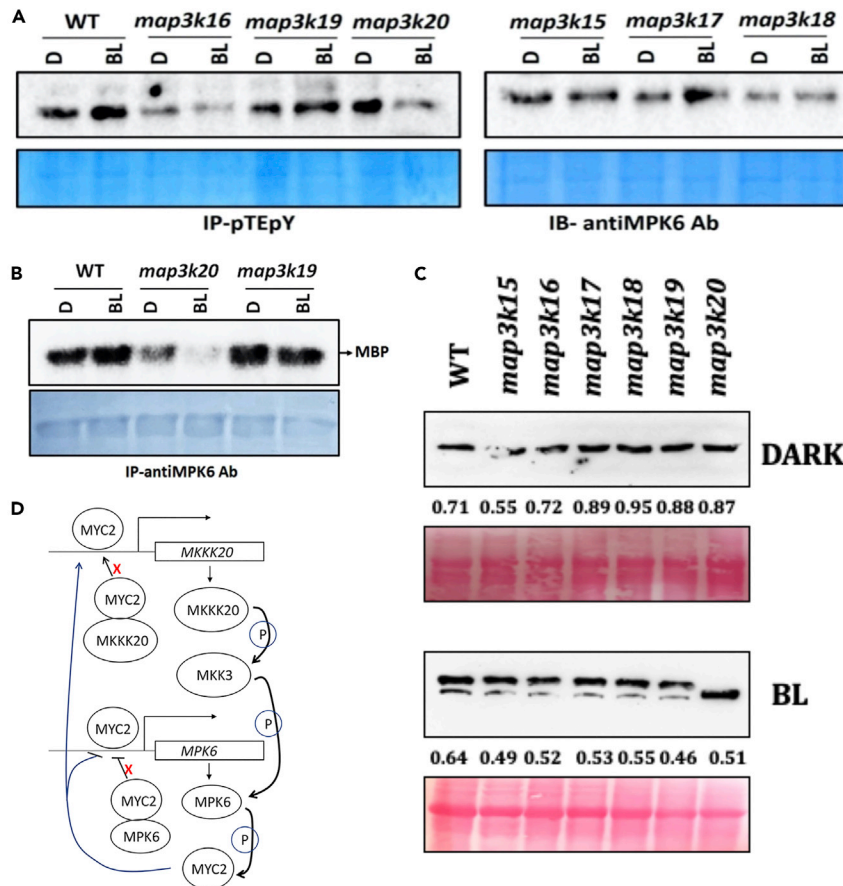
Figure 8. MKKK20 regulates the activity of MPK6

(A) Immunoprecipitation of 10-day-old WT and *map3k* mutant seedlings treated with BL for 10min with pTEpY antibody, followed by immunoblotting with anti-MPK6 antibody to determine the phosphorylation status of MPK6.

(B) Immunoprecipitation of MPK6 from 10-day-old WT and *map3k* mutant seedlings treated with BL for 10min, followed by incubation with MBP as substrate in the kinase reaction mixture to determine kinase activity. All immunoblotting experiments were performed in three independent replicates.

(C) Involvement of MKKK20 in MPK6 phosphorylation after blue light treatment in the seedlings of WT and *map3k* mutants shown by Phos-tag mobility sift assay. Separation of proteins of crude protein extracts of WT and *map3k* mutants after dark and blue light treatments using Phos-tag containing SDS PAGE gel followed by immunoblotting with anti-MPK6 antibody to determine the phosphorylation status of MPK6 by observing the up-sift of phosphorylated protein band. Numbers represent the intensity of MPK6 protein bands relative to Rubisco bands in ponceau staining.

(D) A model showing the MAPK signaling cascade in blue light. The model shows the involvement of MKKK20-MKK3-MPK6 module working upstream to MYC2 in photomorphogenesis. MKKK20 phosphorylates MKK3, which transfers the phosphate moiety to MPK6, which then subsequently phosphorylates MYC2 (Sethi et al., 2014; Benhamman et al., 2017[35,38]; this study). The expression of *MKKK20* is enhanced by MYC2, whereas *MPK6* expression is inhibited by MYC2. MYC2-mediated regulation of expression of *MKKK20* and *MPK6* is nullified by the physical interaction of MYC2 with MKKK20 and MPK6, respectively.

To test the specific role of MKKK20 upstream to MKK3-MPK6-MYC2 module in BL, we examined the phosphorylation status of MPK6 in *mkkk20* and various other *map3k* mutants in BL. For this experiment, wild type, *mkkk15*, *mkkk16*, *mkkk17*, *mkkk18*, *mkkk19* and *mkkk20* seedlings were grown in constant dark for 6-day and then exposed to BL for 10 min. The homozygosity of all the mutants was examined by genotyping PCR using allele specific primers (Figure S7A). Firstly, the phosphorylation status of MPK6 in *map3k* mutant was analyzed by immunoprecipitating the crude protein extract of the seedlings with pTEpY antibody, which specifically interacts with phosphorylated MAPKs.[38] Subsequently, the immunoblot experiment was performed using anti-MPK6 antibody to detect the phosphorylated MPK6. MPK6 phosphorylation level was increased on BL in wild type seedlings (Figure 8A, left panel). Although the level of

phosphorylation of MPK6 remained similar in dark and BL in *mkkk15* to *mkkk19*, the level of phosphorylation was drastically reduced in *mkkk20* background (Figure 8A, right panel). We also studied the transcript level of *MPK6* in wild type and *map3k* mutant seedlings under dark and blue light conditions to determine whether the variation in protein activity among WT and different *map3k* mutants is the consequence of transcriptional regulation. No significant difference in transcript level of *MPK6* was observed between wild type and *map3k* mutants as well as among different *map3k* mutants under dark and BL treatments (Figure S7B).

Because the phosphorylated MPK6 protein was reduced in *mkkk20* mutants, it was important to determine the activity of MPK6, because increase or decrease in protein level does not always resonate with activity of the protein. To determine the activity, crude protein extract of BL-grown wild type, *mkkk19* and *mkkk20* seedlings was immunoprecipitated with anti-MPK6 antibody, and then the immunoprecipitated sample was used as kinase in *in-vitro* phosphorylation assays. Myelin Basic Protein (MBP) was used as a substrate in *in-vitro* kinase assays. An increase in the activity of MPK6 was observed after BL treatment in wild type background (Figure 8B). Although a drastic reduction was observed in the activity of MPK6 in *mkkk20* mutant, no significant difference in MPK6 activity was found in *mkkk19* (Figure 8B). These results indicate that MKKK20 is specifically involved in the phosphorylation of MPK6. Furthermore, to confirm the involvement of MKKK20 in the phosphorylation of MPK6 under *in vivo* condition, we performed the Phos-tag mobility shift assay using the protein extracts of wild type and different *mkkk* mutants after dark and blue light treatments (Figure 8C). Protein extracts of these seedlings were separated in a phos-tag gel, and western blot analysis of MPK6 protein was carried out using anti-MPK6 antibody. No difference in the mobility of MPK6 protein band was observed in the seedlings of wild type and *map3k* mutants after dark treatment. Although in case of BL treatment, wild type and all the *map3k* mutants except *mkkk20* showed retardation in the mobility of MPK6 protein band (Figure 8C), indicating that phosphorylation of MPK6 was abolished in *mkkk20* background. Taken together, these results suggest that MKKK20 is specifically involved in the phosphorylation of MPK6.

DISCUSSION

This study provides evidences that MKKK20 works as an upstream kinase in MKK3-MPK6-MYC2 module to regulate photomorphogenic growth and gene expression. It has been shown earlier that the MKK3-MPK6 module phosphorylates MYC2, and MYC2 specifically interacts with the *MPK6* promoter to regulate its expression.[38] The present study also reveals a similar feedback regulation between MKKK20 and MYC2 in Arabidopsis seedling development (Figure 8D).

This study reveals that MKKK20 works as a negative regulator of photomorphogenic growth at various wavelengths of light. Thus, the BL specific function of the MKK3-MPK6-MYC2 module is not observed in MKKK20. However, MKKK20 works in a MYC2 dependent manner in MKKK20-MKK3-MPK6-MYC2 module during BL-mediated Arabidopsis seedling development. The genetic studies have also revealed that whereas MYC2 works downstream to MKKK20 in BL, it is likely to work in a branched pathway in WL-mediated photomorphogenic growth (Figure 7).

One plausible reason for MKKK20 being functional at various wavelengths of light might be that being the first component of MAP kinase pathways, MKKK20 can cross-talk with other regulatory proteins (in RL and FRL) working downstream to phytochrome signaling pathways. Consistent with this notion, it has recently been shown that MKK10-MPK6 module can phosphorylate and activate PIF3 in regulating the cotyledon opening in RL.[50] The overlap among the functions of the photoreceptors has already been demonstrated. HY5 works at various wavelengths of light to promote photomorphogenesis.[31,47] HY5 and MYC2 directly interact with each other and work in an antagonistic manner to regulate BL-mediated photomorphogenic growth.[37] Similarly, SPA1, an associated factor of COP1, acts as a negative regulator of photomorphogenesis in FR and also in other wavelengths of light.[23,51,52] On the other hand, the function of another COP1 associated factor, SHORT HYPOCOTYL IN WHITE LIGHT 1 (SHW1), is restricted only to WL.[53,54]

The analyses of *mkkk20* mutants exhibit higher level of chlorophyll and anthocyanin content, and the gene expression studies show that MKKK20 represses the expression of light inducible genes such as *CAB1*, *RBCS-1A* and *CHS1*. Although the expression of various key regulatory genes of light signaling pathways were tested, it was observed that *GBF1, HY5, CAM7* and *SPA1* showed higher level of expression in *mkkk20* background (Figure 2), indicating that MKKK20 negatively regulates the expression of these genes. Thus

overall, MKKK20 appears to be a negative regulator of photomorphogenesis. Both negative and positive regulators intimately work in light signaling pathway.[10] This is likely to be the reason that a master regulator of MAP kinase pathway (MKKK20) triggers the expression of both types of regulators, negative and positive, to maintain the homeostasis of the regulatory pathways and gene expression.

The analysis of adult *mkkk20* plants has revealed delayed flowering time under long-day condition similar to *atmyc2* mutants.[22] These findings suggest that MKKK20 positively regulates the flowering time under long-day conditions. *FLC* encodes a MADS-box protein, which acts as a key repressor of inflorescence by negatively regulating the expression of genes such as *SOC1* and *FT* required to switch the meristem to a reproductive fate.[44–46] The qPCR analyses show the elevated level of *FLC* expression in *mkkk20* mutant, indicating that MKKK20 negatively regulates the expression of *FLC*. Therefore, considering the delayed flowering phenotype of *mkkk20*, it is tempting to speculate that MKKK20-mediated suppression of *FLC* might play an important role in controlling the flowering time (Figure 3F).

Among the multiple MAP3Ks tested in this study, the phosphorylation of MPK6 appears to be specifically carried out by MKKK20 pathway. The immunoprecipitation assay with pTEpY antibody followed by immunoblot analysis with anti-MPK6 antibody demonstrates that the level of phosphorylated MPK6 drastically reduced in *mkkk20* mutant as compared to other MAP3Ks tested in BL (Figure 8A). This is further substantiated by using Phos-tag mobility shift assays where retardation in the mobility of MPK6 protein bands in wild type and all *map3k* mutants except in *mkkk20* was observed (Figure 8C). The retardation in mobility is observed as high molecular weight phosphorylated proteins bind to Phos-tag immobilized in the resolving gel and hence migrate more slowly than the non-phosphorylated proteins.[55]

The DNA-protein interaction studies by ChIP and yeast-one hybrid assays demonstrate that MYC2 directly binds to the G-box (CACGTG) and E-box (CATATG) of the *MKKK20* promoter. The binding of MYC2 to the promoter of its target genes through two *cis*-acting elements has already been reported.[56] It will be interesting to investigate in future whether binding of MYC2 to the promoter of *MKKK20* is influenced by other transcription factors through heterodimer formation. As reported earlier, MYC2 physically interacts with other classes of transcription factors, and the resulted heterodimer binds to the promoter of its target genes to regulate the expression differentially.[24]

It has already been shown that MKK3 phosphorylates MPK6, and MPK6 phosphorylates MYC2.[38] We have shown here that MKKK20 specifically interacts with MKK3 (Figure S6). Furthermore, it has been shown that MKKK20 phosphorylates MKK3.[35] Here, we show that phosphorylation of MPK6 is dependent on MKKK20 (Figure 8C). Therefore, the MKKK20-mediated phosphorylation is likely to be operative through MKK3-MPK6-MYC2 module. MKK3 works as a downstream kinase and specifically interacts with MKKK20 to regulate the root microtubule functions.[35] The protein-protein interaction studies have revealed that MKKK20 and MYC2 physically interact with each other (Figure 6). Thus, whereas MKKK20 regulates the activity of MYC2 by phosphorylation through MKKK20-MKK3-MPK6 module, MYC2 binds to the promoters of *MPK6* and *MKKK20* to regulate their transcription. The IP assays carried out by Sethi et al., 2014 have shown that MKK3 activates MPK6 in BL, and the activation of MPK6 in BL is MYC2 dependent.[38] Therefore, considering the findings of Sethi et al., 2014 and the present study, it is tempting to speculate that MYC2 regulates the expression of *MKKK20* and *MPK6*, and once MYC2 is phosphorylated by MPK6, the phosphorylated MYC2 may physically interact with MPK6 and MKKK20 to regulate the pathway through a feedback regulatory function in BL. The interdependent and independent networks of phosphorylation have been reported in eukaryotes. It has been shown that a complex interdependent phosphorylation network is present to work for ChK2 activity in cellular DNA damage repair.[57] Besides, it has been shown that ERF1 binds to the promoters of *MKKK6* and *MPK5*, whereas MPK5 in turn phosphorylates and activates ERF1.[58] Taken together, this study demonstrates that MKKK20 is the upstream kinase of MKK3-MPK6-MYC2 module that is intimately involved in the regulation of photomorphogenesis.

STAR★METHODS

Detailed methods are provided in the online version of this paper and include the following:

- KEY RESOURCES TABLE
- RESOURCE AVAILABILITY
  - ○ Lead contact

○ Materials availability
○ Data and code availability
● EXPERIMENTAL MODEL AND SUBJECT DETAILS
● METHOD DETAILS
○ Chlorophyll and anthocyanin analyses
○ Quantitative reverse transcriptase PCR (qPCR) analysis
○ Yeast two-hybrid assay
○ Bimolecular Fluorescence Complementation (BiFC) assay
○ Chromatin immunoprecipitation assay (ChIP)
○ Yeast one-hybrid assay
○ In vitro kinase assay
○ Plant protein extraction and immunoblot
○ Immunoprecipitation and immuno-kinase assays
○ Phos-tag mobility shift assay
○ GUS staining
○ Quantification of GUS activity
● QUANTIFICATION AND STATISTICAL ANALYSIS

AUTHOR CONTRIBUTIONS

M.O., D.V., A.K.S., and S.C. designed the research. M.O., D.V., N.C., A.P., P.K.B., A.S., and N.V carried out the experiments. M.O., D.V., A.K.S., and S.C. analyzed the data and wrote the manuscript.

DECLARATION OF INTERESTS

The authors have no competing interests to declare.

REFERENCES

1. Kendrick, R.E., and Kronenberg, G.H.M. (1994). Photomorphogenesis in Plants, 2nd edition (Kluwer Academic Publishers).

2. Lin, C. (2002). Blue light receptors and signal transduction. Plant Cell 14 (Suppl), s207–s225.

3. Quail, P.H. (2002). Phytochrome photosensory signalling networks. Nat. Rev. Mol. Cell Biol. 3, 85–93.

4. Jiao, Y., Lau, O.S., and Deng, X.W. (2007). Light-regulated transcriptional networks in higher plants. Nat. Rev. Genet. 8, 217–230.

5. Li, X., Wang, Q., Yu, X., Liu, H., Yang, H., Zhao, C., Liu, X., Tan, C., Klejnot, J., Zhong, D., and Lin, C. (2011). Arabidopsis cryptochrome 2 (CRY2) functions by the photoactivation mechanism distinct from the tryptophan (trp) triad-dependent photoreduction. Proc. Natl. Acad. Sci. USA 108, 20844–20849.

6. Rizzini, L., Favory, J.J., Cloix, C., Faggionato, D., O'Hara, A., Kaiserli, E., Baumeister, R., Schäfer, E., Nagy, F., Jenkins, G.I., and Ulm, R. (2011). Perception of UV-B by the Arabidopsis UVR8 protein. Science 332, 103–106.

7. Chen, M., and Chory, J. (2011). Phytochrome signaling mechanisms and the control of plant development. Trends Cell Biol. 21, 664–671.

8. Tilbrook, K., Arongaus, A.B., Binkert, M., Heijde, M., Yin, R., and Ulm, R. (2013). The UVR8 UV-B photoreceptor: perception, signaling and response. Arabidopsis Book 11, e0164. https://doi.org/10.1199/tab.0164.

9. Ma, L., Li, J., Qu, L., Hager, J., Chen, Z., Zhao, H., and Deng, X.W. (2001). Light control of Arabidopsis development entails coordinated regulation of genome

expression and cellular pathways. Plant Cell *13*, 2589–2607.

10. Jiao, Y., and Deng, X.W. (2007). A genome-wide transcriptional activity survey of rice transposable element-related genes. Genome Biol. *8*, R28.

11. Rodriguez, M.C.S., Petersen, M., and Mundy, J. (2010). Mitogen-activated protein kinase signaling in plants. Annu. Rev. Plant Biol. *61*, 621–649.

12. Liu, Y., and Zhang, S. (2004). Phosphorylation of 1-aminocyclopropane-1-carboxylic acid synthase by MPK6, a stress-responsive mitogen-activated protein kinase, induces ethylene biosynthesis in Arabidopsis. Plant Cell *16*, 3386–3399.

13. Nakagami, H., Pitzschke, A., and Hirt, H. (2005). Emerging MAP kinase pathways in plant stress signalling. Trends Plant Sci. *10*, 339–346.

14. Zhang, A., Jiang, M., Zhang, J., Tan, M., and Hu, X. (2006). Mitogen-activated protein kinase is involved in abscisic acid-induced antioxidant defense and acts downstream of reactive oxygen species production in leaves of maize plants. Plant Physiol. *141*, 475–487.

15. Brodersen, P., Petersen, M., Bjørn Nielsen, H., Zhu, S., Newman, M.A., Shokat, K.M., Rietz, S., Parker, J., and Mundy, J. (2006). Arabidopsis MAP kinase 4 regulates salicylic acid- and jasmonic acid/ethylene-dependent responses via EDS1 and PAD4. Plant J. *47*, 532–546.

16. Takahashi, F., Yoshida, R., Ichimura, K., Mizoguchi, T., Seo, S., Yonezawa, M., Maruyama, K., Yamaguchi-Shinozaki, K., and Shinozaki, K. (2007). The mitogen-activated protein kinase cascade MKK3-MPK6 is an important part of the jasmonate signal transduction pathway in Arabidopsis. Plant Cell *19*, 805–818.

17. Lee, J.S., Wang, S., Sritubtim, S., Chen, J.G., and Ellis, B.E. (2009). Arabidopsis mitogen activated protein kinase MPK12 interacts with the MAPK phosphatase IBR5 and regulates auxin signaling. Plant J. *57*, 975–985.

18. Wang, J., Ding, H., Zhang, A., Ma, F., Cao, J., and Jiang, M. (2010). A novel mitogen-activated protein kinase gene in maize (Zea mays), ZmMPK3, is involved in response to diverse environmental cues. J. Integr. Plant Biol. *52*, 442–452.

19. Sinha, A.K., Jaggi, M., Raghuram, B., and Tuteja, N. (2011). Mitogen-activated protein kinase signaling in plants under abiotic stress. Plant Signal. Behav. *6*, 196–203.

20. Danquah, A., de Zélicourt, A., Boudsocq, M., Neubauer, J., Frei Dit Frey, N., Leonhardt, N., Pateyron, S., Gwinner, F., Tamby, J.P., Ortiz-Masia, D., et al. (2015). Identification and characterization of an ABA-activated MAP kinase cascade in Arabidopsis thaliana. Plant J. *82*, 232–244.

21. Teige, M., Scheikl, E., Eulgem, T., Dóczi, R., Ichimura, K., Shinozaki, K., Dangl, J.L., and Hirt, H. (2004). The MKK2 pathway mediates cold and salt stress signaling in Arabidopsis. Mol. Cell *15*, 141–152.

22. Yadav, V., Mallappa, C., Gangappa, S.N., Bhatia, S., and Chattopadhyay, S. (2005). A basic Helix-Loop-Helix transcription factor in Arabidopsis, MYC2, acts as repressor of Blue Light-mediated photomorphogenic growth. Plant Cell *17*, 1953–1966.

23. Gangappa, S.N., Prasad, V.B.R., and Chattopadhyay, S. (2010). Functional interconnection of MYC2 and SPA1 in the photomorphogenic seedling development of Arabidopsis. Plant Physiol. *154*, 1210–1219.

24. Maurya, J.P., Sethi, V., Gangappa, S.N., Gupta, N., and Chattopadhyay, S. (2015). Interaction of MYC2 and GBF1 results in functional antagonism in blue light-mediated Arabidopsis seedling development. Plant J. *83*, 439–450.

25. Anderson, J.P., Badruzsaufari, E., Schenk, P.M., Manners, J.M., Desmond, O.J., Ehlert, C., Maclean, D.J., Ebert, P.R., and Kazan, K. (2004). Antagonistic interaction between abscisic acid and jasmonate-ethylene signaling pathways modulates defense gene expression and disease resistance in Arabidopsis. Plant Cell *16*, 3460–3479.

26. Boter, M., Ruíz-Rivero, O., Abdeen, A., and Prat, S. (2004). Conserved MYC transcription factors play a key role in jasmonate signaling both in tomato and Arabidopsis. Genes Dev. *18*, 1577–1591.

27. Lorenzo, O., Chico, J.M., Sánchez-Serrano, J.J., and Solano, R. (2004). JASMONATE-INSENSITIVE1 encodes a MYC transcription factor essential to discriminate between different jasmonate-regulated defense responses in Arabidopsis. Plant Cell *16*, 1938–1950.

28. Giri, M.K., Gautam, J.K., Rajendra Prasad, V.B., Chattopadhyay, S., and Nandi, A.K. (2017). Rice MYC2 (OsMYC2) modulates light-dependent seedling phenotype, disease defence but not ABA signalling. J. Biosci. *42*, 501–508.

29. Popescu, S.C., Popescu, G.V., Bachan, S., Zhang, Z., Seay, M., Gerstein, M., Snyder, M., and Dinesh-Kumar, S.P. (2007). Differential binding of calmodulin-related proteins to their targets revealed through high-density Arabidopsis protein microarrays. Proc. Natl. Acad. Sci. USA *104*, 4730–4735.

30. Kushwaha, R., Singh, A., and Chattopadhyay, S. (2008). Calmodulin7 plays an important role as transcriptional regulator in Arabidopsis seedling development. Plant Cell *20*, 1747–1759.

31. Abbas, N., Maurya, J.P., Senapati, D., Gangappa, S.N., and Chattopadhyay, S. (2014). Arabidopsis CAM7 and HY5 physically interact and directly bind to the HY5 promoter to regulate its expression and thereby promote photomorphogenesis. Plant Cell *26*, 1036–1052.

32. Senapati, D., Kushwaha, R., Dutta, S., Maurya, J.P., Biswas, S., Gangappa, S.N., and Chattopadhyay, S. (2019). COP1 regulates the stability of CAM7 to promote photomorphogenic growth. Plant Direct *3*, e00144.

33. Basu, R., Dutta, S., Pal, A., Sengupta, M., and Chattopadhyay, S. (2021). Calmodulin7: recent insights into emerging roles in plant development and stress. Plant Mol. Biol. *107*, 1–20.

34. Kim, J.M., Woo, D.-H., Kim, S.-H., Lee, S.-Y., Park, H.Y., Seok, H.Y., Chung, W.S., and Moon, Y.H. (2012). Arabidopsis MKKK20 is involved in osmotic stress response via regulation of MPK6 activity. Plant Cell Rep. *31*, 217–224.

35. Benhamman, R., Bai, F., Drory, S.B., Loubert-Hudon, A., Ellis, B., and Matton, D.P. (2017). The Arabidopsis mitogen-activated protein kinase kinase kinase 20 (MKKK20) acts upstream of MKK3 and MPK18 in two separate signaling pathways involved in root microtubule functions. Front. Plant Sci. *8*, 1352.

36. Li, K., Yang, F., Zhang, G., Song, S., Li, Y., Ren, D., Miao, Y., and Song, C.P. (2017). AIK1, A mitogen-activated protein kinase, modulates abscisic acid responses through the MKK5-MPK6 kinase cascade. Plant Physiol. *173*, 1391–1408.

37. Chakraborty, M., Gangappa, S.N., Maurya, J.P., Sethi, V., Srivastava, A.K., Singh, A., Dutta, S., Ojha, M., Gupta, N., Sengupta, M., et al. (2019). Functional interrelation of MYC2 and HY5 plays an important role in Arabidopsis seedling development. Plant J. *99*, 1080–1097.

38. Sethi, V., Raghuram, B., Sinha, A.K., and Chattopadhyay, S. (2014). A mitogen-activated protein kinase cascade module, MKK3-MPK6 and MYC2, is involved in blue light-mediated seedling development in Arabidopsis. Plant Cell *26*, 3343–3357.

39. Alonso, J.M., Stepanova, A.N., Leisse, T.J., Kim, C.J., Chen, H., Shinn, P., Stevenson, D.K., Zimmerman, J., Barajas, P., Cheuk, R., et al. (2003). Genome-wide insertional mutagenesis of Arabidopsis thaliana. Science *301*, 653–657.

40. Ilag, L.L., Kumar, A.M., and Söll, D. (1994). Light regulation of chlorophyll biosynthesis at the level of 5-aminolevulinate formation in Arabidopsis. Plant Cell *6*, 265–275.

41. Albert, N.W., Lewis, D.H., Zhang, H., Irving, L.J., Jameson, P.E., and Davies, K.M. (2009). Light-induced vegetative anthocyanin pigmentation in petunia. J. Exp. Bot. *60*, 2191–2202.

42. Zhang, H.N., Li, W.C., Wang, H.C., Shi, S.Y., Shu, B., Liu, L.Q., Wei, Y.Z., and Xie, J.H. (2016). Transcriptome profiling of light-regulated anthocyanin biosynthesis in the pericarp of litchi. Front. Plant Sci. *7*, 963.

43. Mallappa, C., Singh, A., Ram, H., and Chattopadhyay, S. (2008). GBF1, a transcription factor of blue light signaling in Arabidopsis, is degraded in the dark by a proteasome-mediated pathway independent of COP1 and SPA1. J. Biol. Chem. *283*, 35772–35782.

44. Michaels, S., and Amasino, R. (1999). FLOWERING LOCUS C encodes a novel MADS domain protein that acts as a repressor of flowering. Plant Cell *11*, 949–956.

45. Sheldon, C.C., Burn, J.E., Perez, P.P., Metzger, J., Edwards, J.A., Peacock, W.J., and Dennis, E.S. (1999). The FLF MADS box gene: a repressor of flowering in Arabidopsis regulated by vernalization and methylation. Plant Cell *11*, 445–458.

46. Deng, W., Ying, H., Helliwell, C.A., Taylor, J.M., Peacock, W.J., and Dennis, E.S. (2011). FLOWERING LOCUS C (FLC) regulates development pathways throughout the life cycle of Arabidopsis. Proc. Natl. Acad. Sci. USA *108*, 6680–6685.

47. Ang, L.H., Chattopadhyay, S., Wei, N., Oyama, T., Okada, K., Batschauer, A., and Deng, X.W. (1998). Molecular interaction between COP1 and HY5 defines a regulatory switch for light control of Arabidopsis development. Mol. Cell *1*, 213–222.

48. Srivastava, A.K., Dutta, S., and Chattopadhyay, S. (2019). MYC2 regulates ARR16, a component of cytokinin signaling pathways, in Arabidopsis seedling development. Plant Direct *3*, e00177.

49. Kiba, T., Yamada, H., and Mizuno, T. (2002). Characterization of the ARR15 and ARR16 response regulators with special reference to the cytokinin signaling pathway mediated by the AHK4 histidine kinase in roots of Arabidopsis thaliana. Plant Cell Physiol. *43*, 1059–1066.

50. Xin, X., Chen, W., Wang, B., Zhu, F., Li, Y., Yang, H., Li, J., and Ren, D. (2018).

Arabidopsis MKK10-MPK6 mediates red-light-regulated opening of seedling cotyledons through phosphorylation of PIF3. J. Exp. Bot. *69*, 423–439.

51. Saijo, Y., Sullivan, J.A., Wang, H., Yang, J., Shen, Y., Rubio, V., Ma, L., Hoecker, U., and Deng, X.W. (2003). The COP1-SPA1 interaction defines a critical step in phytochrome A-mediated regulation of HY5 activity. Genes Dev. *17*, 2642–2647.

52. Seo, H.S., Watanabe, E., Tokutomi, S., Nagatani, A., and Chua, N.H. (2004). Photoreceptor ubiquitination by COP1 E3 ligase desensitizes phytochrome A signaling. Genes Dev. *18*, 617–622.

53. Bhatia, S., Gangappa, S.N., Kushwaha, R., Kundu, S., and Chattopadhyay, S. (2008b). Short hypocotyl in white light (SHW1), a serine-arginine-aspartate-rich protein in Arabidopsis, acts as a negative regulator of photomorphogenic growth. Plant Physiol. *147*, 169–178.

54. Srivastava, A.K., Senapati, D., Srivastava, A., Chakraborty, M., Gangappa, S.N., and Chattopadhyay, S. (2015). Short hypocotyl in white light1 interacts with elongated hypocotyl5 (HY5) and constitutive photomorphogenic1 (COP1) and promotes COP1-mediated degradation of HY5 during Arabidopsis seedling development. Plant Physiol. *169*, 2922–2934.

55. Li, H., Ding, Y., Shi, Y., Zhang, X., Zhang, S., Gong, Z., and Yang, S. (2017). MPK3- and MPK6-mediated ICE1 phosphorylation negatively regulates ICE1 stability and freezing tolerance in Arabidopsis. Dev. Cell *43*, 630–642.e4.

56. Zhang, Q., Xie, Z., Zhang, R., Xu, P., Liu, H., Yang, H., Doblin, M.S., Bacic, A., and Li, L. (2018). Blue light regulates secondary cell wall thickening via MYC2/MYC4 activation of the NST1-directed transcriptional network in Arabidopsis. Plant Cell *30*, 2512–2528.

57. Guo, X., Ward, M.D., Tiedebohl, J.B., Oden, Y.M., Nyalwidhe, J.O., and Semmes, O.J. (2010). Interdependent phosphorylation within the kinase domain T-loop Regulates CHK2 activity. J. Biol. Chem. *285*, 33348–33357.

58. Schmidt, R., Mieulet, D., Hubberten, H.M., Obata, T., Hoefgen, R., Fernie, A.R., Fisahn, J., San Segundo, B., Guiderdoni, E., Schippers, J.H.M., and Mueller-Roeber, B. (2013). Salt-responsive ERF1 regulates reactive oxygen species-dependent signaling during the initial response to salt stress in rice. Plant Cell *25*, 2115–2131.

59. Bradford, M.M. (1976). A rapid and sensitive method for the quantitation of microgram quantities of protein utilizing the principle of protein-dye binding. Anal. Biochem. *72*, 248–254.

60. Jefferson, R.A., Kavanagh, T.A., and Bevan, M.W. (1987). GUS fusions: b-glucuronidase as a sensitive and versatile gene fusion marker in higher plants. EMBO J. *6*, 3901–3907.

61. Block, M., and Debrouwer, D. (1992). In situ enzyme histochemistry on plastic embedded plant material. The development of an artifact-free p-glucuronidase assay. Plant J. *2*, 261–266.

STAR★METHODS

KEY RESOURCES TABLE

REAGENT or RESOURCE	SOURCE	IDENTIFIER
Antibodies		
Rabbit Anti- MPK6	Sigma-Aldrich	Cat#A7104 RRID: AB_476760
Rabbit Anti- pTEpY	Cell signaling	Cat# 4370 RRID: AB_2315112
Rabbit polyclonal anti-c-Myc	Sigma-Aldrich	Cat#C3956 RRID: AB_439680
Bacterial and virus strains		
DH5α	N/A	N/A
BL21(DE3)pLysS	N/A	N/A
GV3101	N/A	N/A
Chemicals, peptides, and recombinant proteins		
Glutathione Sephasose	GE Healthcare	Cat#17075605
Ni-NTA Agarose	BR-BiochemLifeSciences	Cat#BCBSP079
Dyna beads Protein A	Invitrogen	Cat#10002D
Dyna beads Protein G	Invitrogen	Cat#10004D
Protease Inhibitor cocktail	Sigma-Aldrich	Cat#p9599
Phos-tag Acrylamide	AAL-107 Nard Institute, Ltd	Cat#AAL-107
Critical commercial assays		
5-bromo-4-chloro-3-indolyl-b-D-glucuronic acid	Sigma-Aldrich	Cat#B6650
4-Methylumbelliferyl-b-D-glucuronide hydrate	Sigma-Aldrich	Cat#M9130
ATP	Sigma-Aldrich	Cat#A6559
Experimental models: Organisms/strains		
Arabidopsis *mkkk15*	ABRC	SALK_102721C Genebank: N666898
Arabidopsis *mkkk16*	ABRC	SALK_003255C Genebank: N660683
Arabidopsis *mkkk17*	ABRC	SALK_080309C Genebank: N675893
Arabidopsis *mkkk18*	ABRC	CS877670 Genebank: N877670
Arabidopsis *mkkk19*	ABRC	CS825913 Genebank: N825913
Arabidopsis *mkkk20*	ABRC	SALK_124398 Genebank: N624398
Arabidopsis *mpk6*	ABRC	CS31099 Genebank: N31099
Arabidopsis *myc2*	ABRC	CS428097 Genebank: N428097
Arabidopsis *mkk3*	ABRC	CS66016 Genebank: N66016
Arabidopsis *pMKKK20:GUS*	This Paper	N/A
Arabidopsis *MYC2OE*	This Paper	N/A

(Continued on next page)

Continued		
REAGENT or RESOURCE	SOURCE	IDENTIFIER
Oligonucleotides		
See Table S1 in Supplemental information	Sigma-Aldrich	Custom Order
Recombinant DNA		
pMKKK20:GUS	This Paper	N/A
pSPYCE: MYC2-cYFP	This Paper	N/A
pSPYNE: MKKK20-nYFP	This Paper	N/A
BD-MYC2	This Paper	N/A
AD-MKKK20	This paper	N/A
Software and algorithms		
Image J	National Institutes of Health	1.48u

RESOURCE AVAILABILITY

Lead contact

Requests for resources and reagents should be written to and will be fulfilled by the Lead Contact, Alok Krishna Sinha (alok@nipgr.ac.in).

Materials availability

This study did not generate new material.

Data and code availability

- This paper uses existing, publicly available data. The accession numbers for the genotypes used, are listed in the key resources table.

- This paper does not report original code.

- Any additional information reported in this paper is available from the lead contact upon request.

- List of primers used in the study is mentioned in Table S1.

EXPERIMENTAL MODEL AND SUBJECT DETAILS

The wild-type *A. thaliana* and mutants used in this study are in Columbia (Col-0) background. The transfer DNA insertion *mkkk20* mutant lines (SALK_124398, SALK_021755) has been ordered from Arabidopsis Biological Research Center (ABRC). The homozygosity for *mkkk20* mutants were confirmed by Genomic PCR analysis. Primers used for genomic PCR and to detect the exact position of transfer DNA, are gene specific left primer (LP), gene specific reverse primer (RP), and transfer DNA specific left border primer (transfer DNA LBP). The other mutant lines used in this study are: *mkkk15* (SALK_102721C); *mkkk16* (SALK_003255C); *mkkk17* (SALK_080309C); *mkkk18* (CS877670); *mkkk19* (CS825913). The seeds were surface sterilized (using sodium hypochlorite, Triton X-100) and plated on Murashige and Skoog basal medium (MS plates) with 1% sucrose. The plates were then kept at 4° in darkness for 4 days to allow stratification prior to germination of the seeds. After stratification the plates were transferred in to the Arabidopsis growth chamber at a maintained temperature of $21 \pm 2°C$ with the required wavelength and intensity of light. For phenotypic study, the 6 days old seedlings were used for hypocotyl length measurements using ImageJ (Fiji) 1.41 software. The intensities of light were used for WL (10 $\mu mol\ m^{-2}\ s^{-1}$), blue light (20 $\mu mol\ m^{-2}\ s^{-1}$), red light (20 $\mu mol\ m^{-2}\ s^{-1}$) and far-red light (1.5 $\mu mol\ m^{-2}\ s^{-1}$). Adult *Arabidopsis* plants were grown under a long day (LD) condition with 14h of white light and 10h of darkness (14 h L/10 D).

METHOD DETAILS

Chlorophyll and anthocyanin analyses

Chlorophyll and Anthocyanin contents were estimated as described in Yadav et al.(2005).[22]

Quantitative reverse transcriptase PCR (qPCR) analysis

Total RNA was isolated from the 6-day-old seedlings grown under respective light conditions using RNeasy plant mini kit (Qiagen). Reverse transcription was performed from 1 μg of total RNA using Thermo Scientific RevertAID H Minus First Strand cDNA synthesis Kit followed by qPCR using Power SYBR Green PCR Master Mix (Applied Biosystems). For qPCR gene specific primers were used. The *ACTIN2* was used as reference gene to normalize the qPCR values.

Yeast two-hybrid assay

The yeast two-hybrid assays were carried out following the Matchmaker GAL4 Two-Hybrid System (Clontech, USA). To generate constructs for yeast two-hybrid assays, the full length CDS of MYC2 was cloned in pGBKT7 vector using *NdeI* and *PstI* restriction enzymes to produce GAL4 DNA-binding domain (BD) fused MYC2 as bait protein. Similarly, the full length CDS of MKKK20 was cloned in pGADT7 vector using *EcoRI* and *BamHI* restriction enzymes to produce GAL4 Activating domain (AD) fused MKKK20 as prey protein. The constructs were co-transformed into *AH109* yeast strain following small scale LiAC transformation Clontech protocol. The co-transformed *AH109* yeast colonies were selected on synthetic double drop-out plate (2D) devoid of Leucine and Tryptophan (-Leu,-Trp). Then the protein-protein interaction was studied by examining the growth of the transformed colonies on synthetic quadruple drop-out plate (4D) devoid of Leucine, Tryptophan, Histidine, Adenine (- Leu,-Trp,-His,-Ade).

Bimolecular Fluorescence Complementation (BiFC) assay

For the BiFC studies, full length CDS of MYC2 was cloned in pSPYCE vector using *SpeI* and *KpnI* restriction enzymes to generate MYC2-YFP^{C-ter} (MYC2-cYFP) and full length CDS of MKKK20 was cloned in pSPYNE-35S vector using *SpeI* and *KpnI* restriction enzymes to generate MKKK20 -YFP^{N-ter} (MKKK20-nYFP). All the constructs along with pBin-HC-Pro (Helper plasmid) were transformed individually into *Agrobacterium GV3101* strain. The *Agrobacterium* strain harboring the respective constructs were mixed in a ratio 1:1:1 and allowed it to co-express in onion epidermal cells following the protocol described in Xu et al., 2014. Reconstitution of YFP was identified by yellow fluorescence underLeica TCS SP8 Confocal laser scanning microscope (Leica microsystems, Germany). Empty BiFC vectors (cYFP + nYFP) and their combinations with MYC2- cYFP (MYC2-cYFP + nYFP) and MKKK20-nYFP (MKKK20-nYFP + cYFP) were co-expressed in onion epidermal cells as negative controls.

Chromatin immunoprecipitation assay (ChIP)

The ChIP assays were performed as described by Gangappa et al. (2010) with some modifications.[23] Six-day-old blue light (30 μmol/m^2/s^1) grown wild type and transgenic MYC2OE seedlings were used for the experiment. The anti-*c*-Myc antibody (Sigma-Aldrich) was used for the immunoprecipitation. The immuno-precipitated products were subjected to real-time PCR analysis for monitoring the enrichment of the promoter fragment using *MKKK20* promoter-specific primers and non-box primers. For real-time PCR analysis, we have used Power SYBR® Green PCR Master Mix (Applied Biosystems).

Yeast one-hybrid assay

To perform Yeast One-Hybrid assay, 750 bp of the promoter fragment having G-box and E-box was used. We have cloned 750 bp promoter fragment in the pLazZi2μm vector using EcoRI and XhoI restriction sites. The DNA fragment containing the mutated E-box, mutated G-box, and both mutated E-box and G-box were constructed by primer-based site-directed mutagenesis using the same restriction sites and vector mentioned above. MYC2 full-length CDS was cloned in AD-vector using NdeI and ClaI. All the constructs, including negative controls, were co-transformed into *EGY48* yeast strain following Clontech small scale LiAc transformation protocol and plated on double dropout (2D) plate devoid of Leucine and Uracil. Transformed colonies on 2D plate were selected and re-streaked on Leucine and Uracil devoid plate but supplemented with X-gal substrate to check the interaction of the questioned protein to the promoter fragment.

In vitro kinase assay

In-vitro activation assay was done according to the method described by Takahashi et al. (2007).[16] Protein (Kinase or phosphatase and substrate) were incubated in 10 μL of kinase reaction buffer (50 mM Tris–HCl, pH 7.5, 1 mM DTT, 10 mM $MgCl_2$, 10 mM $MnCl_2$, 50 mM ATP, and 0.037 MBq of (γ32P ATP) [60 Ci/mmol]) at 30°C for 30min. Kinase reactions were stopped after 30min by adding 2X SDS loading dye and heating for

5 minat 95°C. Reaction products were run on SDS-PAGE gel, and were analyzed by autoradiography, and Coomassie Brilliant Blue R 250 staining.

Plant protein extraction and immunoblot

Crude plant protein extract was isolated from Arabidopsis seedlings using kinase extraction buffer (50 mM HEPES (pH 7.5), 5 mM EDTA, 5 mM EGTA, 10 mM dithiothreitol, 10 mM Na_3VO_4, 10 mM NaF, 50 mM β-glycerolphosphate, 1 mM phenylmethylsulfonyl fluoride, protease inhibitor cocktail, 10% glycerol) and were quantified using Bradford assay.[59]

Approximately, 30 μg of plant protein was run on 12% SDS-PAGE until front dye reached bottom of the gel. Stacked gel was removed and the resolved gel was kept in transfer buffer. Nylon-P was pre-wetted in absolute methanol for 15–20min and the gel was equilibrated in transfer buffer for 10 min. The transfer stack was assembled by first keeping sponge pad on the surface of *trans* blot semi dry transfer cell (Biorad, USA) followed by 2–3 layers of wet Whatman filter papers. PVDF membrane was placed on the Whatman filter paper. Equilibrated gel was positioned on the PVDF membrane and gel surface was wetted with a few drops of transfer buffer. The remaining filter papers (2–3) were laid on the gel and air bubbles were removed using glass rod by rolling, this was followed by layering with sponge. The assembly was closed and transfer was carried out at 25 mA for 1h. After run, membrane was stained with Ponceau stain and washed with water. The membrane was kept in blocking buffer for overnight at 4°C and washed thrice with washing buffer (TBST) for 10min each. After washing, the membrane was incubated with primary antibody for 1hat dilution 1:15,000. The membrane was again washed with TBST for 10min 3 times and incubated with secondary antibody at dilution 1:15,000 in blocking solution for 1h. Membrane was washed with TBST and signal was detected using Supersignal west Pico chemiluminescent substrate (Pierce, USA).

Immunoprecipitation and immuno-kinase assays

For Immunoprecipitation, 300 μg of crude protein was incubated anti-pTEpY antibody (Cell Signaling Technology, Danvers, MA, USA; catalog #9101) or rabbit polyclonal anti-MPK6 antibody (Sigma, catalog #A7104) along with protein A Sepharose beads (Sigma). For this, protein A Sepharose beads were firstly pre-equilibrated using 1X PBS buffer followed by incubation with appropriate amount of anti-pTEpY or anti-MPK6 antibody in an Eppendorf tube rotator at 4°C. After ∼5 h, antibody-beads complexes were washed thrice with 1X PBS buffer and incubated with plant extract for ∼5 h on an Eppendorf tube rotator at 4°C. Finally, the beads containing antibody bound plant protein were washed with 1X PBS buffer and used as sample for Western blotting or kinase assay. For immuno-kinase assay, samples were incubated with MBP as substrate, in a reaction mixture containing 25 mM Tris/HCl (pH 7.5), 10 mM $MgCl_2$, 5 mM $MnCl_2$, 1 mM DTT, 1 mM β-glycerol-phosphate, 1M Na_3VO_4, 0.5 μg/mL MBP, 25 μM ATP, and1μCi [$\gamma^{-32}P$] ATP) and incubated at 30°C for 30 min. Finally, 5μLof 5X SDS sample buffer was added, samples were boiled at 95°C for 5 min, and then separated in 15% SDS/PAGE gel. The radioactive gels were visualized using phos-phor imager (Typhoon, Phosphor Imaging System, GE Health Care, Life Sciences, USA).

Phos-tag mobility shift assay

Phos-tag mobility shift assay was performed using the Phos-tag reagent (NARD Institute) as described by Li et al. (2017).[55] Proteins were extracted from the seedlings and resolved in 8% SDS-PAGE gel having 40 μM Phos-tag and 100 mM $MnCl_2$. After electrophoresis, the gel was washed three times for 10 min each using the transfer buffer containing 10 mM EDTA and finally with the transfer buffer without EDTA for 10 min, and then the resolved proteins were transferred to nitrocellulose membrane. Anti MPK6 antibody (sigma) was used to detect MPK6 protein.

GUS staining

Histochemical staining for GUS activity in transgenic plants was performed as described by Jefferson et al. (1987) and DeBlock and DeBrouwer (1992).[60,61] Different tissues of transgenic plants were harvested and immediately immersed in the reaction solution composed of 1 mM 5-bromo-4-chloro-3-indolyl-b-D-glucuronic acid, 50 mM sodium phosphate, 1 mM ferricyanide, 1 mM ferrocyanide and 0.1% Triton X-100, pH 7.0. After 5 min of vacuum infiltration, samples were incubated overnight at 37°C. Chlorophyll of stained tissues was bleached by serial washes of decreasing concentrations of ethanol (from 90% to 50%), each for 30 min and pictures of the stained tissues were taken with a stereomicroscope.

Quantification of GUS activity

Total protein from the tissue was extracted in GUS extraction buffer followed by protein quantification by Bradford's method.[59] Flourometric GUS assays using 4-methylumberrifyl-β-glucuronide (MUG) substrate were performed according to a method described by Jefferson et al. (1987).[60] The product 4-methylumbelliferone (MU) of reaction was quantitated at excitation wavelength of 360 nm and emission wavelength of 460 nm. GUS activity was recorded for two time points one for 10 and another for 20 min for each sample. GUS activity was calculated as pmol MU/min/mg protein.

QUANTIFICATION AND STATISTICAL ANALYSIS

Quantification of proteins was carried out by quantifying the intensity of protein bands using ImageJ. Three independent replicates of each experiment were performed. Data was presented in the form of mean of three replicates $\pm$ SD. Significant difference between two groups of data was calculated using one-way ANOVA factorial analysis followed by Tukey's HSD test and Student's T test.